Extinction and the Radial Distribution of Supernova Properties in Their Parent Galaxies

KAZUHITO HATANO, DAVID BRANCH, AND JENNIFER DEATON

Department of Physics and Astronomy, University of Oklahoma, Norman, OK 73019

Received _____; accepted _____

ABSTRACT

We use a Monte Carlo technique and assumed spatial distributions of dust and supernova (SN) progenitors in a simple model of a characteristic SN–producing disk galaxy to explore the effects of extinction on the radial distributions of SN properties in their parent galaxies. The model extinction distributions and projected radial number distributions are presented for various SN types. Even though the model has no core–collapse SNe within three kpc of the center, a considerable fraction of the core–collapse SNe are projected into the inner regions of inclined parent galaxies owing to their small vertical scale height. The model predicts that because of extinction, SNe projected into the central regions should on average appear dimmer and have a much larger magnitude scatter than those in the outer regions. In particular, the model predicts a strong deficit of bright core-collapse events inside a projected radius of a few kpc. Such a deficit is found to be present in the observations. It is a natural consequence of the characteristic spatial distributions of dust and core–collapse SNe in galaxies, and it leads us to offer an alternative to the conventional interpretation of the Shaw effect.

Subject headings: dust, extinction — galaxies: ISM — supernovae: general

1. Introduction

Inferring the true radial dependence of supernova (SN) properties in their parent galaxies from observations of projected radial distributions is a tricky business. For example, Bartunov, Makarova, and Tsvetkov (1992) could find no significant difference between the radial distributions of SNe of Type Ia (SNe Ia) and Type II (SNe II) in disk galaxies, while van den Bergh (1997) and Wang, Höflich, & Wheeler (1997) reach opposite conclusions as to whether SNe Ia or SNe II are more centrally concentrated. Wang et al also conclude that SNe Ia farther than 7.5 kpc from the centers of their parent galaxies are more homogeneous in absolute magnitude and $B - V$ color than those that are closer to the centers. An obvious and generally recognized difficulty in this kind of work is that only the projected distance of an SN from the center of its galaxy, not the true distance, is observed. Another difficulty, that to our knowledge has not previously been explored, is that extinction of SNe by dust in their parent galaxies can affect the observed radial dependence of SN properties.

To make a first exploration of the effects of extinction on the radial dependence of SN properties, we have used a Monte Carlo technique together with assumed spatial distributions of dust and SN progenitors in a simple model of a characteristic SN–producing disk galaxy. The model is described in section 2, and the extinction distributions and projected radial distributions that it predicts for the various SN types are presented. Model predictions of how the brightness distributions of the various SN types depend on projected radius are presented and compared with observation in section 3. Section 4 presents a brief discussion.

2. The Model

2.1. Input

Our Monte Carlo technique for studying the visibility of SNe and novae (Hatano et al. 1997a,b,c) was inspired by a study of the visibility of Galactic SNe by Dawson and Johnson (1994). In their model and in Hatano et al. (1997a,b), which were concerned with SNe and novae in the Galaxy, a double exponential distribution of dust was used, with a radial scale length of five kpc and a vertical scale height of 0.1 kpc. Core–collapse events (SNe II and Ibc) were distributed like the dust except that they were not allowed to occur within three kpc of the center in view of the lack of evidence for much recent star formation in the central regions of our Galaxy. SNe Ia consisted of two spatially interpenetrating components: disk SNe Ia had a double exponential distribution with a scale length of five kpc and a vertical scale height of 0.35 kpc and they were not truncated at three kpc. Bulge SNe Ia were spherically distributed (in kpc) as $(R^3 + 0.7^3)^{-1}$. Disk SNe Ia outnumbered bulge SNe Ia by a factor of seven, consistent with the estimated Galactic disk–to–bulge mass ratio (van der Kruit 1990). The bulge was truncated at three kpc and the disk at 20 kpc. For more detailed descriptions of the model, see Dawson and Johnson (1994) and Hatano et al. (1997a).

Hatano et al. (1997c) was concerned with novae in M31. Because the dust density in M31 is known to peak not at the center, but well out in the disk where most of the current star formation is taking place, the model dust distribution was modified accordingly. Recently Sodroski et al. (1997) have found that in the Galaxy, too, the dust density peaks off center, at a radius of about 5 kpc, where the total face–on extinction through the disk is $A_B \simeq 1$. For the present study we have made a simple parameterization of the radial dependence of the total face–on extinction through the disk, after Figure 9 of Sodrowski et al. This radial dependence of the dust, together with a retained vertical scale height of 0.1 kpc, leads to the following expression for the B–band extinction per kpc, α, in the plane

of the disk:

$$\alpha(r) = r, \quad r \leq 5 \text{ kpc}, \tag{1}$$

$$\alpha(r) = -0.4r + 7, \quad r > 5 \text{ kpc} \tag{2}$$

Thus the dust density rises from zero at the center of the model to a maximum value at 5 kpc and then falls to zero at 17.5 kpc. This particular parameterization gives a rather high value of 3.8 mag kpc^{-1} in the plane of the disk at $r = 8$ kpc, i.e., at the radial distance of the sun in the Galaxy, but considering that large galaxies produce more SNe and tend to be more dusty than small ones (van den Bergh & Pierce 1990), it probably is not unreasonable for this initial exploration of the effects of extinction.

2.2. Model Extinction Distributions

Figure 1 shows the model extinction distributions for bulge SNe Ia, disk SNe Ia, and core–collapse SNe, each for five different galaxy inclinations as well as for a random distribution of inclinations. Note that for any inclination, even edge–on, the distributions for bulge and disk SNe Ia are strongly peaked at small values of $A_B \leq 0.1$. (For the adopted disk–to–bulge SN Ia ratio of seven, the total distribution for SNe Ia is much like the distribution for disk SNe Ia.) Core–collapse SNe tend to be more extinguished than SNe Ia owing to their smaller vertical scale height.

Table 1 quantifies the model extinction distributions. Column (1) gives the cosine of the inclination of the model, where $\cos(i) = 1$ refers to the face–on case. Columns (2)–(4) refer to bulge SNe Ia (Ia–b) and list the mean extinction $< A_B >$, the mean extinction of an "extinction–limited subset" of bulge SNe Ia that have $A_B < 0.6$, and the fraction of the events in that subset. Columns (5)–(7) give the same information for disk SNe Ia

(Ia–d) and columns (8)–(10) are for core–collapse SNe (CC). In the edge–on case the mean extinction of all SN types becomes high, but of course there would be a strong observational selection acting against the discovery of severely extinguished events. It is interesting that the mean extinction of the extinction–limited subsets *decreases* as inclination increases, i.e., when the model is highly inclined the extinction tends to be all or nothing. Note that even in the edge–on case substantial fractions of bulge and disk SNe Ia make it into the extinction–limited subsets, while only a small fraction of the core–collapse SNe do. Column (10) shows that, to the extent that an extinction of 0.6 mag is sufficient to significantly reduce the probability that a SN is discovered, this particular model is dusty enough to support an inclination–dependent observational discrimination against the discovery of core–collapse SNe (cf. van den Bergh 1993; Tammann 1994; Cappellaro & Turatto 1997).

2.3. Model Projected Radial Distributions

Our technique allows us to plot model projected radial distributions of SNe for comparison with observed distributions. The model distributions presented here have been calculated with a disk truncation radius of 30 rather than 20 kpc because some SNe have been observed beyond 20 kpc.

Figure 2 shows normalized projected radial distributions for disk SNe Ia and core–collapse SNe, for five inclinations and a random distribution of inclinations. As the inclination increases, the projected distributions shift toward the central regions. The behavior of the core–collapse SNe is especially interesting: in the face–on case, by construction, there are no core–collapse events within three kpc, but in the edge–on case plenty are projected into the innermost regions because of the small vertical scale height. This illustrates that the observational presence of core–collapse events projected near the center does not guarantee the actual existence of core–collapse events near the center. More

generally, Figure 2 illustrates the difficulty of inferring details about the relative radial distributions of SN types from observations of their projected radial distributions in samples that include highly inclined galaxies, especially if the SN types have different vertical scale heights.

van den Bergh (1997) studied projected SN radial distributions in a sample of disk galaxies restricted to those having $i < 70^o$, to minimize extinction and projection effects, and he tentatively concluded that SNe Ia are more centrally concentrated than SNe II. Wang et al (1997) presented calculated projected radial distributions, analagous to our Figure 3 but with very different model parameters. They compared to observed distributions and tentatively concluded the opposite — that SNe II are more centrally condensed than SNe Ia. Because Wang et al. did not use a smaller vertical scale height for SNe II than for SNe Ia, they probably overestimated the true central concentration of SNe II relative to that of SNe Ia; thus it appears to us that van den Bergh's conclusion is more likely to be correct.

3. The Radial Dependence of SN Brightness

At this point we have to specify the SN luminosity functions. After Hatano et al (1997a) we adopt gaussian distributions of the intrinsic absolute magnitudes of SNe Ia, Ibc, and II, with mean absolute magnitudes of -19.5, -18.0, and -17.0, and dispersions of 0.2, 0.3, and 1.2, respectively.

3.1. Type Ia Supernovae

The top panel of Figure 3 shows the model distribution of absolute magnitude as viewed by the external observer who has not corrected for parent–galaxy extinction (i.e., the quantity $M_B + A_B$) for SNe Ia. Those at large projected radial distances are practically

unextinguished, while some of those at smaller projected distances are severely extinguished. The lower panel of Figure 3 shows a corresponding observational plot, constructed from data in the June 6, 1997 version of the Asiago Supernova Catalogue with distances based on parent–galaxy radial velocity and $H_0 = 60$ km s^{-1} Mpc^{-1}. Apparent magnitudes have been corrected for foreground extinction in the Galaxy but not for extinction in the parent galaxies. Considering the simplicity of our model, and that the lower panel is affected by strong observational bias against the discovery of severely extinguished events, the general resemblance of the two panels of Figure 3 is satisfactory. Figure 3 strongly suggests that the effects of parent–galaxy extinction are likely to be the cause of much of the observed difference in absolute–magnitude dispersion between SNe Ia within and beyond 7.5 kpc, a difference first pointed out by Wang et al. (1997). It should be noted, however, that for a small sample of SNe Ia having high–quality data, Wang et al. also found an excess of *overluminous* SNe Ia within 7.5 kpc, which of course cannot be explained in terms of extinction. Wang et al also called attention to an apparent observational deficit of SNe Ia in the innermost one kpc of their parent galaxies. The upper panel of Figure 3 shows that our model predicts the presence of observationally bright SNe Ia (mostly bulge SNe Ia) projected into the central kpc, while none appear in the observational plot (lower panel of Figure 3). This supports the suggestion by Wang et al. that bulge populations may be poor producers of SNe Ia. (The conclusion of Wang et al that SNe Ia therefore do not come from novae does not follow for us, because we [Hatano et al. 1997b,c] have argued that Galactic and even M31 novae do not come primarily from the bulge populations as is usually assumed.)

3.2. Core–Collapse Supernovae

Figure 4 is like Figure 3, but for SNe II. Although the effects of the broad adopted luminosity function for SNe II are apparent, the upper panel of Figure 4 shows the same general tendency as Figure 3 for many severely extinguished model SNe to appear at relatively small projected distances from the center. (Some are extinguished right off the top of Figure 4.) The large triangle in the upper panel serves to call attention to predicted deficit of bright SNe II in the central regions. In the model the deficit reflects the tendency of SNe II that are projected into the central regions to be substantially extinguished. Although more data are needed to reach a final conclusion, this deficit does appear to be present in the observations (lower panel). In the same way the model predicts a deficit of bright SNe Ibc in the central regions, and the inset to the lower panel shows that although the numbers are still smaller, observations of SNe Ibc are at least consistent with the presence of the deficit.

We have explored the consequences for the core–collapse deficit of altering the dustiness of the model. Halving the dustiness makes the model deficit less pronounced than the observational one, while doubling the dustiness extinguishes nearly all centrally projected core–collapse SNe beyond detectability. Measuring the radial dependence of controlled samples of SNe in galaxies appears to be a promising way to constrain the amount and the distribution of dust in galaxies, which is a controversial issue (Valentijn 1990; Burstein, Haynes, & Faber 1991).

The results shown in Figure 4 lead us to suggest an alternative to the classical explanation of the selection effect discussed by Shaw (1979) — the observational deficit of SNe in the central regions of remote galaxies relative to nearer galaxies. (See van den Bergh (1997) and Wang et al (1997) for plots that illustrate the Shaw effect with present data.) Shaw's interpretation, which has been generally accepted, was that the effect is

caused by the increasing difficulty, with distance, of discovering SNe against the bright central regions of galaxies. But if this is the primary cause of the Shaw effect then in Figure 4 we would expect to see a deficit of observationally *dim* SNe in the central regions, because they would be more readily lost than bright ones. Then the large triangle in the lower panel of Figure 4 should be upside down. Instead, the lower panel of Figure 4 shows a deficit of observationally *bright* SNe II in the central regions, as predicted by our model. Therefore we suggest that the Shaw effect for SNe II (and SNe Ibc) comes about at least in part because core–collapse SNe projected into the central regions of galaxies tend to be observationally dim, and the difficulty of discovering dim SNe increases with distance. Our model does not predict such a deficit for SNe Ia, but it is not so clear that there really is an observational Shaw effect for SNe Ia (see Figure 3 of van den Bergh [1997] and Figure 1 of Wang et al [1997]).

4. Discussion

Our simple model of the spatial distributions of dust and SN progenitors in a characteristic SN–producing disk galaxy predicts that owing to extinction, SNe projected into the inner regions of their parent galaxies tend to be observationally dimmer and to have a much larger magnitude dispersion than SNe in the outer regions. As Wang et al (1997) first showed, such is the case for SNe Ia. In our model the effect is severe enough, for core–collapse SNe, to produce a deficit of observationally bright events projected into the central regions. For core–collapse SNe, such a deficit does appear to be present in the observational data. Although the need for improving on the assumption of a single characteristic SN–producing disk galaxy in future work is obvious, this effect of extinction is likely to be real. It has obvious implications for such things as using high–redshift SNe Ia to determine the cosmic deceleration (avoid extinction by using events in the outer

regions of their parent galaxies); for determining the true relative radial distributions of SN types (extinction can cause confusion, especially when comparing SN types that have different vertical scale heights), and for determining SN rates (substantial corrections for incompleteness that depend on parent–galaxy dustiness are required).

Adam Fisher wrote the original version of our Monte Carlo code. We are grateful to Eddie Baron, Darrin Casebeer, Dean Richardson, Bill Romanishin, and Rollin Thomas for many discussions in the course of this work, which was supported by NSF grant AST 9417102. J.D. was supported in part by an NSF REU Supplement to AST 9417242.

REFERENCES

Bartunov, O. S., Makarova, I. N., and Tsvetkov, D. Yu. 1992, A&A, 264, 428

Burstein, D., Haynes, M. P., and Faber, S. M. 1991, Nature, 353, 515

Cappellaro, E. & Turatto, M. 1997, in Thermonuclear Supernovae, ed. R. Ruiz–Lapuente, R. Canal, & J. Isern (Dordrecht: Kluwer), 77

Dawson, P. C. & Johnson, R. G. 1994, J. R. Astron. Soc. Can., 88, 369

Hatano, K., Fisher, A., and Branch, D. 1997a, MNRAS, 290, 360

Hatano, K., Branch, D., Fisher, A., and Starrfield, S. 1997b, MNRAS, 290, 113

Hatano, K., Branch, D., Fisher, A., and Starrfield, S. 1997c, ApJL, 487, L45

Shaw, R. L. 1979, A&A, 76, 188

Sodroski, T. J., Odegard, N., Arendt, R. G., Dwek, E., Weiland, J. L., Hauser, M. G., & Kelsall, T. 1997, ApJ, 480, 173

Tammann, G. A. 1994, in Supernovae, ed. S. A. Bludman, R. Mochkovitch, & J. Zinn–Justin (Amsterdam: North Holland), 1

Valentijn, E. A. 1990, Nature, 346, 153

van den Bergh, S. 1993, Comments Ap., 17, 125

van den Bergh, S. 1997, AJ, 113, 197

van den Bergh, S. & Pierce, M. J. 1990, ApJ, 364, 444.

van der Kruit, P. 1990, in The Milky Way as a Galaxy, ed. R. Buser & I. King (Mill Valley: University Science Books), 331

Wang, L., Höflich, P., and Wheeler, J. C. 1997, ApJ, 483, L29

This manuscript was prepared with the AAS LaTeX macros v4.0.

Fig. 1.— The model A_B distributions for (a) bulge SNe Ia; (b) disk SNe Ia; and (c) core–collapse SNe, each for five inclinations of the model. The inclinations are equally spaced in cos(i). The thick solid lines are the A_B distributions for a random distribution of inclinations.

Fig. 2.— Normalized model projected radial distributions of disk SNe Ia and core–collapse SNe, for five inclinations and for random inclinations. Line legends are as Figure 1.

Fig. 3.— *upper*: The model distribution of $M_B + A_B$ for SNe Ia plotted against the projected radial distance from the center of the model. The distribution of inclinations is random, with symbols as follows: cos(i) = 1 – filled circle; cos(i) = 0.75 – asterisk; cos(i) = 0.5 – square; cos(i) = 0.25 – diamond; and cos(i) = 0, triangle. The horizontal line corresponds to the mean of the adopted intrinsic absolute–magnitude distribution for SNe Ia and the dashed vertical line as at one kpc *lower*: The corresponding observed distribution based on data from the Asiago Supernova Catalogue. Open circles denote peculiar SNe Ia, two of which are intrinsically red.

Fig. 4.— Like Figure 3, but for SNe II. In the upper panel, symbols are as in Figure 3. In the lower panel, squares denote SNe II–P, filled circles denote SNe II–L, open circles denote peculiar SNe II. The large triangles call attention to the predicted and observed deficits of observationally bright SNe II in the central regions. The inset in the bottom panel is for observed SNe Ibc. Circles denote SNe Ib and squares denote SNe Ic.

Table 1. Extinction of Various Supernova Types

(1)	(2)	(3)	(4)	(5)	(6)	(7)	(8)	(9)	(10)
	Ia–b	Ia–b	Ia–b	Ia–d	Ia–d	Ia–d	CC	CC	CC
cos(i)	$< A_B >$	$< A_B >$	f(Ia–b)	$< A_B >$	$< A_B >$	f(Ia–d)	$< A_B >$	$< A_B >$	f(CC)
1.00	0.12	0.12	1.00	0.30	0.16	0.76	0.32	0.24	0.84
0.75	0.18	0.14	0.92	0.40	0.15	0.65	0.41	0.24	0.71
0.50	0.36	0.13	0.72	0.58	0.14	0.55	0.62	0.24	0.54
0.25	1.06	0.08	0.46	1.17	0.13	0.43	1.21	0.22	0.34
0.00	4.26	0.07	0.52	8.80	0.12	0.32	19.8	0.14	0.07

Fig 1

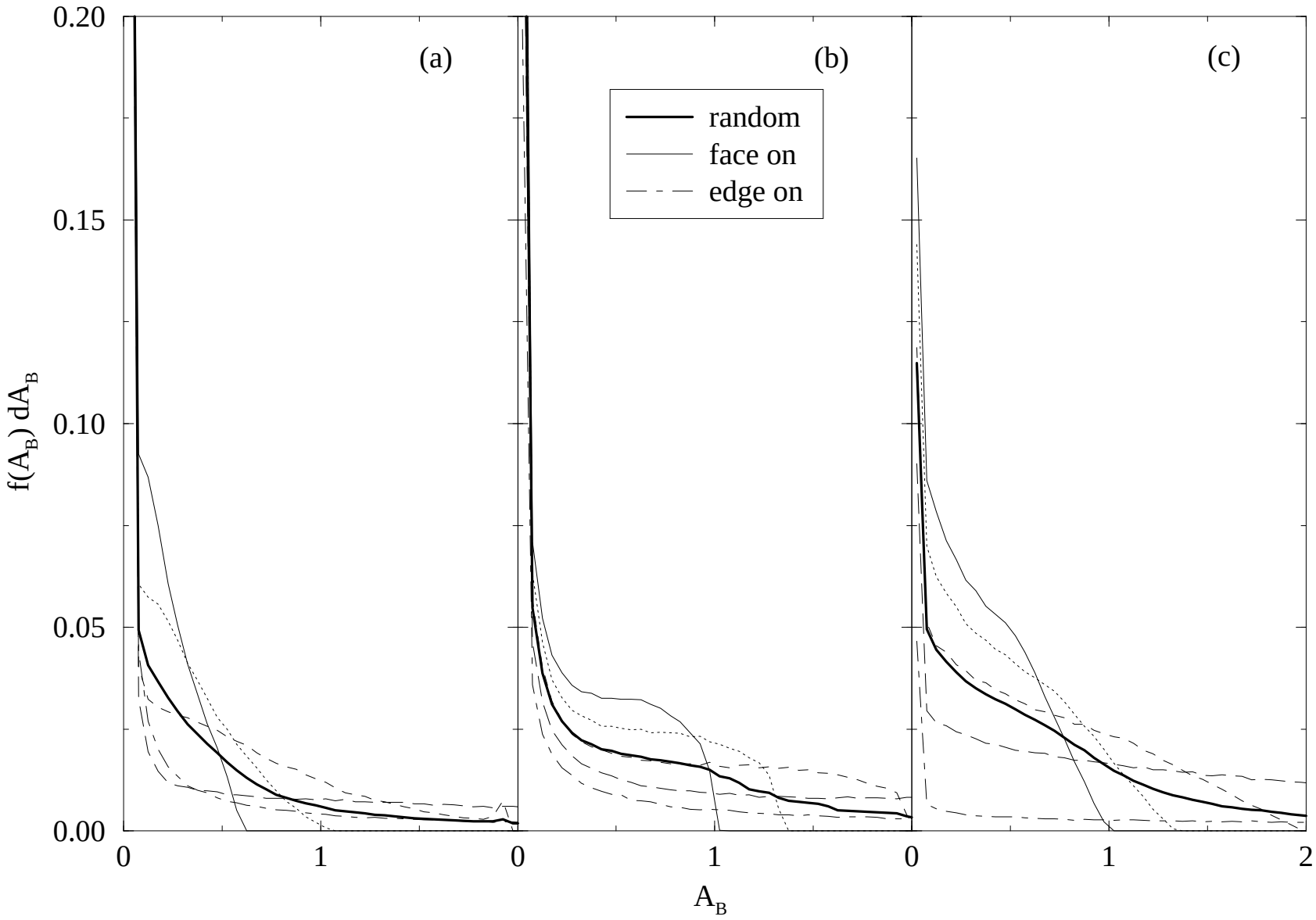
0.20
0.15
0.10
0.05
0.00
f(A_B) dA_B
(a)
(b)
(c)
random
face on
edge on
0
1
0
1
0
1
2
A_B

Fig 2

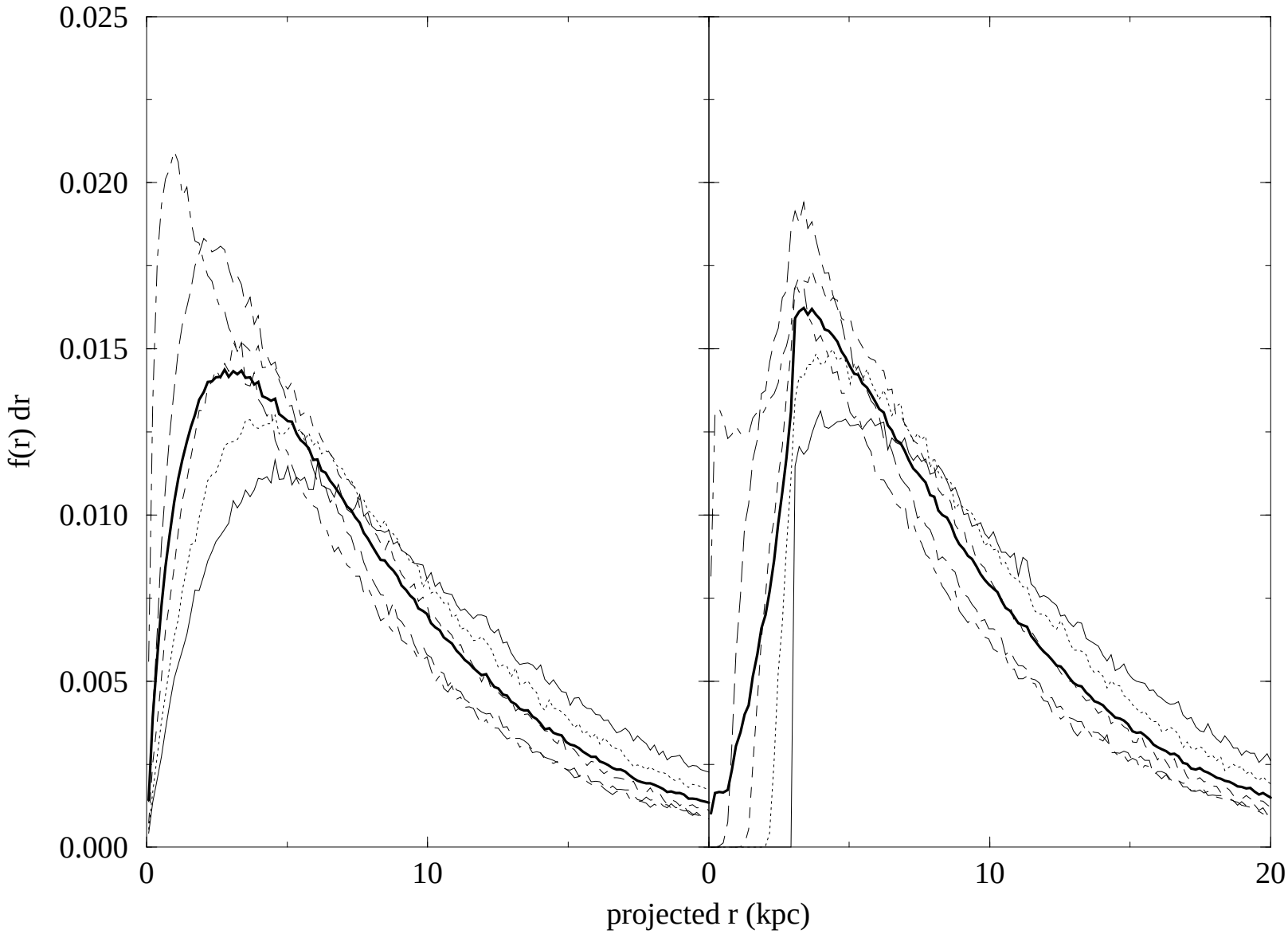

Fig 3

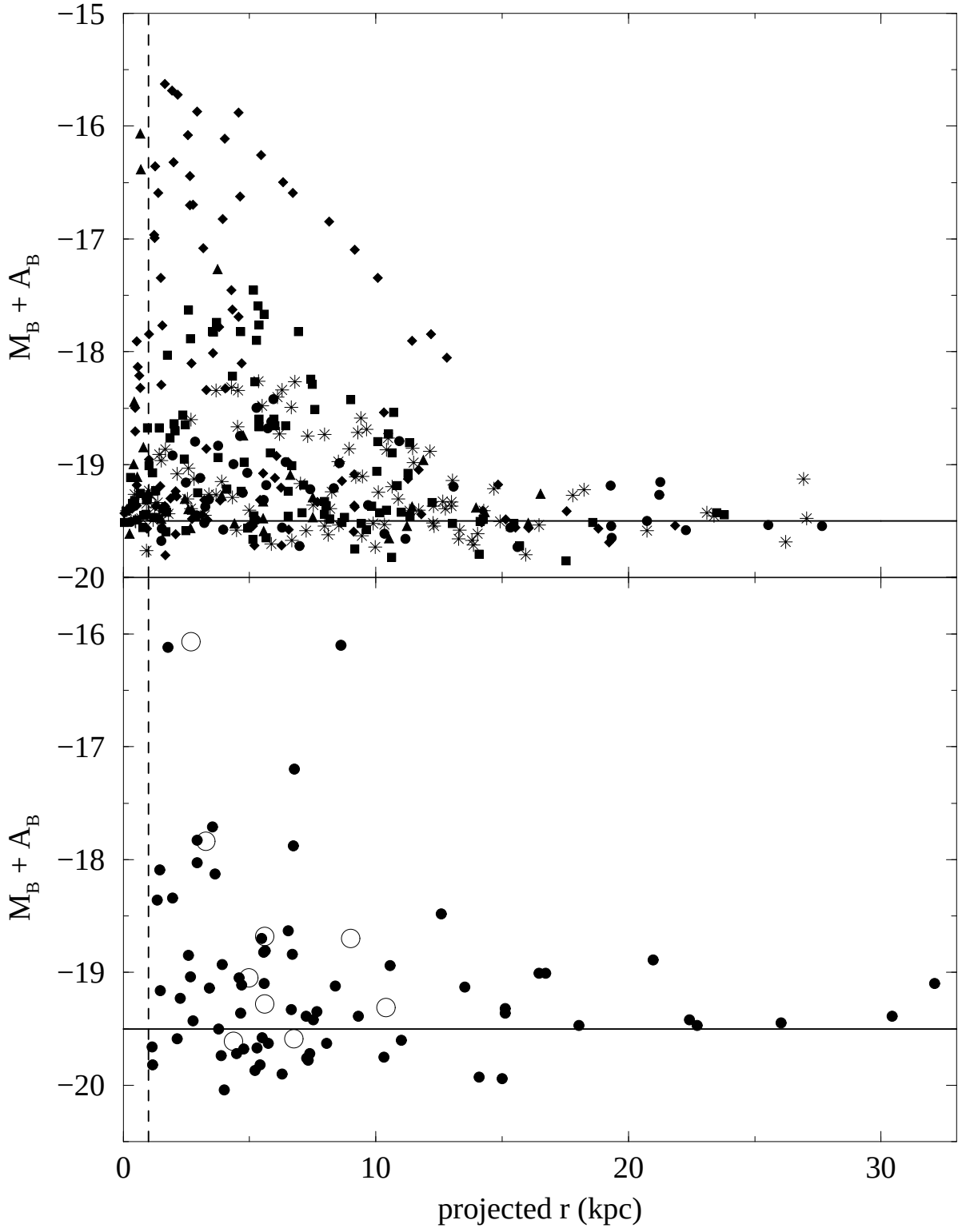
−15
−16
−17
−18
−19
−20
$M_B + A_B$
−16
−17
−18
−19
−20
$M_B + A_B$
0
10
20
30
projected r (kpc)

Fig 4